Uncertainty Quantification in 3D Imaging of Atmospheric Dispersion Processes with Dial

Absorption-based Optical Imaging of Dispersion Processes

Robert Lung, Nick Polydorides

University of Edinburgh

April 2022

Differential Absorption based Imaging

Basics Working Principle

Problem: Determine the 3D spatial concentration profile of a known trace gas using differential absorption Lidar.

- Measure (back-)scattered light at wavelengths, λ_{on} and λ_{off}, with identical scattering but different absorption by the trace gas.
- 3D imaging requires scan of a cone. ($\rightarrow$ Lidar cube)
- Additional atmospheric data is sometimes necessary or useful.

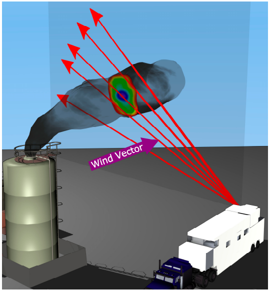

Mobile Lidar scanning a plume cross section[1]

[1] Illustration taken from Innocenti, F and Robinson, R and Gardiner, T and Finlayson, A and Connor, A. Differential Absorption Lidar (DIAL) measurements of landfill methane emissions, *Remote Sensing*, 2017.

Differential Absorption based Imaging

Wide vs. Narrow FOV

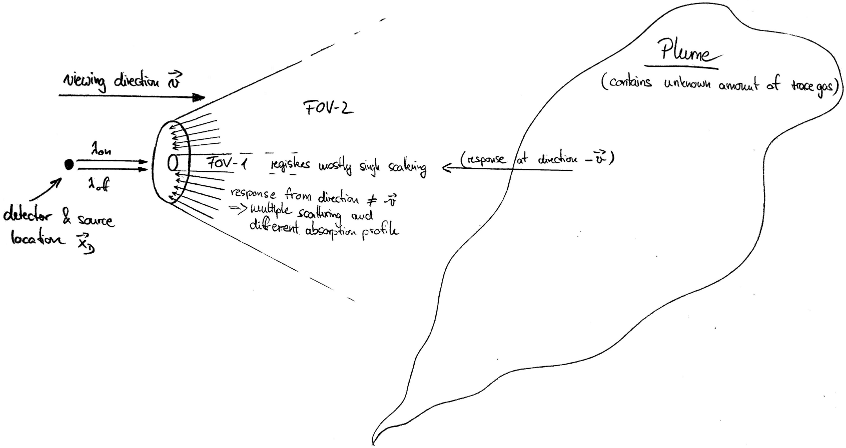

Figure: FOV-1 captures a very narrow cone and thus light that corresponds mostly to single scattering. The wider FOV-2 captures light that scattered multiple times which isn't modelled by the Lidar equation and doesn't have the same absorption profile as single scattering.

The two ingredients
Radiative Transfer

- The dynamics of light in heterogeneous scattering media can be modelled via the Radiative Transfer Equation (RTE)

$$\left(\frac{\partial}{\partial t} + v \cdot \nabla_x + \sigma_a^{\text{on/off}} + \sigma_s\right) H^{\text{on/off}} = \sigma_s \int_{\mathbb{S}^2} H^{\text{on/off}} f_p \mathrm{d}v'$$

  where $\sigma_s, \sigma_a^{\text{on/off}}$ are heterogeneous scattering/absorption parameters and f_p is a phase function.

- The source term is $\delta(v - v_j)\delta(t)$ and differs for each direction v_j within the scanned cone.
- The measurement is taken **at a single point** on the boundary separately for each v_j.

The two ingredients
Low-dimensional Dispersion

- We consider the advection-diffusion equation given by

$$\frac{\partial}{\partial t}u + \nabla \cdot (\eta u) - Q + \frac{1}{2}\nabla \cdot (\kappa \nabla u) = 0 \qquad (1)$$

with $Q = \rho_Q \cdot \delta(\vec{x} - \vec{q})\delta(t)$ is an instantaneous source term at $\vec{q}$ while η, κ model drift and diffusion respectively and shall be functions of time only.

- The plume can be modelled as a superposition of puffs ϕ

$$\sum_{j=1}^{N} w_j \phi \left(\frac{\|x - m_j\|_2}{h_j} \right) \qquad (2)$$

for w_j, h_j and m_j which depend on the dispersion quantities and **regularise the inverse problem by imposing PDE based constraints**.

Parameter Uniqueness under RTE Assumption

Single vs. Multiple Scattering

For functions such as (2) we can exploit the existence of a "first impact point" and use that single scattering is more singular and can be measured earlier than higher order scattering to show:

Theorem (uniqueness)

Assuming the optical forward model is governed by the RTE, then, given σ_a, σ_s and f_p, a differential absorption field $\sigma_a^{\text{on}} - \sigma_a^{\text{off}}$ of akin to the form (2) is, for continuous optical parameters, uniquely determined by the on and off intensities regardless of the field-of-view.

In other words, given the scattering, there is only a difference between wide and narrow FOVs when we consider noisy data:

- Discrepancies between the average model used in the inverse problem and the true concentration profile
- Optical noise due to limited photon counts in each bin

Optical Problem

Likelihood and noise

Poisson noise model for the optical yields log-likelihood for data binned at mid-points t_i

$$\mathsf{L}(\theta \mid \boldsymbol{m}, \boldsymbol{n}) = \sum_{i,j} H^{\text{on}}(t_i, v_j) + H^{\text{off}}(t_i, v_j) - \boldsymbol{m}_{v_j,t_i} \log(H^{\text{on}}(t_i, v_j)) - \boldsymbol{n}_{v_j,t_i} \log(H^{\text{off}}(t_i, v_j))$$

where $\theta = (\alpha_\psi, Q_\psi, H^{\text{off}})$ and $H^{\text{on}} = H^{\text{off}} \mathbb{E}_{p \sim Q_\psi}[\alpha_\psi(p)]$

- The effect of high-dimensional scattering parameters is captured within H^{off} while α, Q are parameterised by low-dimensional dispersion related parameters ψ.
- Closed form solutions for H^{off} alongside low-dimensionality of gradients lead to tractable reconstruction process.

Optical Problem

Parameter fitting

Maximum of $\mathsf{L}(\cdot \mid \boldsymbol{m}, \boldsymbol{n})$ w.r.t. H^{off} is at $H^{\text{off}}_{\psi} = \frac{\boldsymbol{m}_{v_j,t_i} + \boldsymbol{n}_{v_j,t_i}}{1+\mathbb{E}_{p\sim Q_{\psi}}[\alpha_{\psi}(p)]}$ so we can find ψ by iterating

$$\psi_{r+1} = \psi_r + \mathcal{I}(\psi_r)^{-1}\partial_{\psi}\mathsf{L}(\alpha_{\psi_r}, Q_{\psi_r}, H^{\text{off}}_{\psi_r} \mid \boldsymbol{m}, \boldsymbol{n})$$

and $\mathcal{I}(\psi)$ approximates the Hessian and is of the form

$$\mathcal{I}(\psi) = \sum_{i,j}(\boldsymbol{m}_{v_j,t_i} + \boldsymbol{n}_{v_j,t_i})\left(\frac{\partial_{\psi}P(\psi)\partial_{\psi}P(\psi)^{\mathsf{T}}}{P(\psi)^2} + \frac{\partial_{\psi}P(\psi)\partial_{\psi}P(\psi)^{\mathsf{T}}}{(1-P(\psi))^2}\right)$$

- Only first derivatives! Limits number of RTE evaluations.
- Matrix concentration inequalities provide bounds on approximation quality for approximate RTE evaluations (low-dimensionality of ψ!)

Use a super-position of branching jump diffusion processes to get centres for functions of the form (2) by:

- Making use of Fokker–Planck equation for

$$\mathrm{d}X_t = \eta \mathrm{d}t + \kappa \mathrm{d}B_t$$

  where κ, η as in (1) and B_t standard Wiener process.

- Adjusting kernel weights and widths such that expectation matches that of low-dimensional smooth component
- Taking affine combinations to mimic the empirical observation that "Big whorls have little whorls which have lesser whorls..."

Simulations

Reconstruction of Smooth Image and Parameters of Interest

- Simulated reconstruction from $80 \times 20 \times 50$ Lidar scan of 9 parameter dispersion which can be recovered when conventional reconstruction fails due to the low SNR.
- **The reference point**: Low-dimensional (regularised) vs. High-dimensional (noisy) concentration profiles

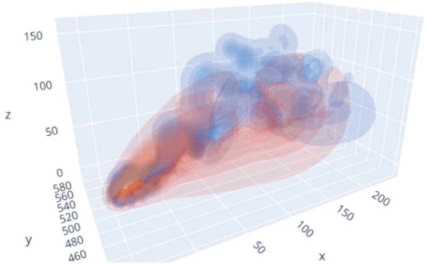

Figure: Low vs. High-dimensional difference ≈ 0.5 relative L_1 error

Simulations

Reconstruction[1] from $80 \times 20 \times 50$ Lidar scan: Release amount ρ_Q

- The parameter that controls the release rate is the ideal case for wide FOVs.
- Most photons are useful and separation of FOVs is of limited use here.

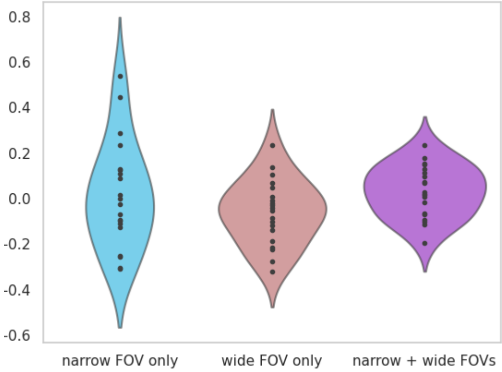

[1] 10 plumes with 2 optical data sets each = 20 runs

Simulations

Reconstruction[1] from $80 \times 20 \times 50$ Lidar scan: Source location $\vec{q}$

- The source parameter controls the overall positioning of the gas plume.
- Most photons are again useful and but separation of FOVs is of use here.
- Different properties of x and y component result in non-isotropic error distribution.

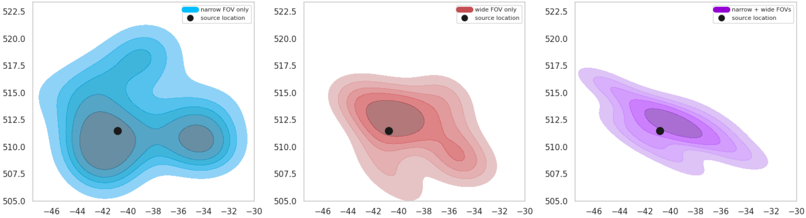

[1] 10 plumes with 2 optical data sets each = 20 runs

The difference in L_1 errors[2] is largely determined by the previous two quantities underlining complex relationship of errors and data.

- Quadratic expansion involving $\mathcal{I}$ under-estimates errors.
- MCMC based approaches can work but require RTE evaluations for high dimensional parameters.
- The non-parametric nature of $\frac{\mathrm{d}H^{\text{on}}}{\mathrm{d}H^{\text{off}}} = E_{p \sim Q_\psi}[\alpha_\psi(p)]$ may be dealt with by considering $\frac{\mathrm{d}H^{\text{on}}}{\mathrm{d}H^{\text{off}}} \approx E_{p \sim Q_\psi}[\alpha_\psi(p)]$.

(pro) Laplace approximations of marginal posterior may be obtained more quickly than MCMC samples.

(con) Hyper-parameters for the distribution of $\frac{\mathrm{d}H^{\text{on}}}{\mathrm{d}H^{\text{off}}}$ to "match" a prior for dispersion are hard to determine.

[2] 0.61, 0.48 and 0.41 respectively